

Effat University Repository

Two-Dimensional DOA Zero-Forcing Precoding for Enhanced Spectral Efficiency in Cell-Free Massive MIMO

Authors	Ali, Ehab;Balfaqih, Mohammed;Shglouf, Ibrahim;Alrayes, Mohamed;Balfagih, Zain
Citation	E. Ali, M. Balfaqih, I. Shglouf, M. Alrayes and Z. Balfagih, "Two-Dimensional DOA Zero-Forcing Precoding for Enhanced Spectral Efficiency in Cell-Free Massive MIMO," 2025 22nd International Learning and Technology Conference (L&T), jeddah, Saudi Arabia, 2025, pp. 164-169, doi: 10.1109/LT64002.2025.10941497. keywords: {Direction-of-arrival estimation;Spectral efficiency;Precoding;Estimation;Interference;Downlink;Vectors;Multiple signal classification;Uplink;Contamination;Zero Forcing Precoding;Cell-free Massive-MIMO;2D-Direction of arrival},
DOI	https://doi.org/10.1109/LT64002.2025.10941497
Publisher	IEEE
Rights	CC0 1.0 Universal
Download date	2026-05-21 10:37:19
Item License	http://creativecommons.org/publicdomain/zero/1.0/
Link to Item	https://repository.effatuniversity.edu.sa/handle/20.500.14131/2261

Two-Dimensional DOA Zero-Forcing Precoding for Enhanced Spectral Efficiency in Cell-Free Massive MIMO

Ehab Ali
University of Benghazi
Benghazi, Libya
ehabalisahli@uob.edu.ly
y

Mohammed Balfaqih
University of Jeddah
Jeddah, Saudi Arabia
mabalfaqih@uj.edu.sa

Ibrahim Shglouf
Libyan International
University
Benghazi, Libya
ibrahim.alshellmani@li.mu.edu.ly

Mohamed Alrayes
University of Tripoli
Tripoli, Libya
mo.alrayes@uot.edu.ly

Zain Balfagih
Effat University
Jeddah, Saudi Arabia
zbalfagih@effatuniversity.edu.sa

Abstract—Energy and spectral efficiency in mobile networks are enhanced by Cell-free Massive-MIMO systems utilizing macro-diversity to optimize overall performance. However, multi-user interference, especially due to pilot reuse within the same cell, continues to pose significant challenges. This research introduces a Two-Dimensional Direction of Arrival (2D-DOA) Zero-Forcing Precoding method. It addresses both intra-cell and inter-cell interference, removing the requirement for Channel State Information exchange between Access Points (APs). A new expression for downlink spectral efficiency is developed, considering the impacts of imperfect CSI and pilot contamination. Utilizing UESPRIT and MUSIC -based 2D-DOA estimation techniques, the proposed method surpasses pilot-contaminated systems and deterministic Zero-Forcing precoding, demonstrating enhanced spectral efficiency even under constrained pilot resources.

Keywords— Zero Forcing Precoding, Cell-free Massive-MIMO, 2D-Direction of arrival.

I. INTRODUCTION

Conventional 5G cellular networks aim for extensive connectivity, minimal delay, and robust dependability, with Massive-MIMO as a key enabler [1-3]. By employing multiple antennas at base stations, Massive-MIMO enhances spatial multiplexing through beamforming, boosting energy and spectral efficiency. However, growing data demands and dense network deployments create challenges, such as inter-cell interference, particularly at cell boundaries. To address these issues, cell-free Massive-MIMO has been proposed, leveraging distributed access points (APs) connected to a central processing unit to enable synchronized service management. Effective channel state information (CSI) estimation remains crucial, but pilot contamination, resulting from the limited availability of orthogonal pilots, continues to hinder performance.

Several approaches have been developed to address pilot contamination, including sophisticated pilot allocation strategies and advanced precoding methodologies. While techniques such as greedy and location-based pilot assignment improve individual user performance, their system-wide effectiveness remains limited [4-6]. Precoding strategies like robust MMSE and rate-splitting have demonstrated improved performance but often come with high complexity, making them impractical for large-scale cell-free networks [7-9].

Recent approaches leverage spatial characteristics, such as the two-dimensional direction of arrival (2D-DOA) precoding, to mitigate intra- and inter-cell interference [10]. By exploiting 2D-DOA information, this method distinguishes between users, improving signal separation and interference mitigation. Techniques like Two-Dimensional

Unitary ESPRIT and 2D Fourier Domain Line Search MUSIC show promising results in mitigating pilot contamination while maintaining spectral efficiency.

Building on these insights, this study emphasizes the uplink and downlink performance of cell-free Massive-MIMO systems in the presence of pilot contamination. A novel uplink estimator is introduced, integrating Direction of Arrival (DOA) information with statistical channel characteristics. For the downlink, a Zero-Forcing precoding approach is employed, leveraging the pseudo-inverse of the channel matrix. Compared to MMSE precoding, Zero-Forcing offers reduced computational complexity and enhanced suitability for dense network environments, effectively mitigating interference while providing straightforward closed-form performance expressions. This method showcases its potential to enhance scalability and interference management in cell-free Massive-MIMO deployments.

II. SYSTEM MODEL

This research explores a cell-free Massive-MIMO system operating in Time Division Duplexing (TDD) mode to exploit channel reciprocity and reduce pilot overhead. The network comprises a single hexagonal cell with L access points (APs), K user equipment (UEs), and M_{xy} antenna elements per AP, arranged in both the x and y directions, ensuring $LM_{xy} \gg K$. All APs are interconnected via front-haul links and are managed by distributed central processing units (CPUs), which handle payload data distribution, downlink power control, and Direction of Arrival (DOA) estimation.

The focus is on a 2D-DOA-based zero-forcing precoding scheme. Zero-forcing precoding is particularly advantageous due to its simplicity and efficacy in suppressing interference, leveraging the pseudo-inverse of the estimated channel matrix to minimize interference. This approach is highly suitable for cell-free Massive-MIMO systems, efficiently managing large numbers of APs and supporting dense user scenarios while benefiting from TDD-enabled channel reciprocity. Each coherence interval block has a duration $t_{c,k}$ and consists of three components: the uplink pilot signal $t_{p,k}$, uplink data transmission $t_{u,k}$, and downlink data transmission $t_{d,k}$, where the total time is given by $t_{c,k} = t_{p,k} + t_{u,k} + t_{d,k}$.

A. Channel Model and Uplink Training

To assess the practical performance of cell-free Massive-MIMO systems, a channel model must accurately reflect the defining characteristics of large-scale networks with numerous access points (APs). Key considerations include the geometric arrangement of APs, the correlation between channel responses across different APs, and the spatial positioning and orientation of both APs and user equipment

(UEs). To model spatial correlation caused by limited antenna spacing and scattering environments, the channel vectors are represented using the Kronecker model, as outlined in prior studies [10], [11]. This correlated channel model is integrated with the Direction of Arrival (DOA) estimation technique to evaluate system performance. The analysis assumes that UEs are either stationary or moving at low speeds, ensuring consistent shadowing and path loss conditions.

During the uplink training phase, active UEs transmit unique pilot sequences to all APs, enabling channel estimation within each coherence interval. The pilot sequence assigned to the k -th UE in the system is expressed as:

$$\mathbf{s}_{l,k} = [s_{l,1} s_{l,2} s_{l,3} \dots s_{l,\tau}]^T \quad (1)$$

Where τ represents the length of the pilot sequence, with $\|\mathbf{s}_k\|^2 = 1$. It is assumed that all pilot sequences are mutually orthogonal, ensuring that:

$$\mathbf{s}_{l,k}^H \mathbf{s}_{l,k} = \begin{cases} 1, & \text{if } \mathbf{s}_{l,k} = \mathbf{s}_{l,k} \\ 0, & \text{if } \mathbf{s}_{l,k} \neq \mathbf{s}_{l,k} \end{cases} \quad (2)$$

The pilot signal captured by AP \mathbf{Y}_l is represented as:

$$\mathbf{Y}_l \triangleq \sum_{k=1}^K h_{l,k} \sqrt{t_u p_{l,k}} \mathbf{s}_{l,k} + \mathbf{N}_l \in \mathbb{C}^{M \times 1} \quad (3)$$

Here, p_k represents the normalized uplink transmit power, $\mathbf{N}_l \in \mathbb{C}^{M \times 1}$ denotes the Gaussian noise matrix, and M is the total number of access points. The spatial correlation matrices incorporate steering vectors corresponding to various 2D-Direction of Arrival (DOA) angles for the k^{th} user. The channel vector representing the connection between user k and access point l is defined in [12] and can be expressed as:

$$h_{l,k} = \frac{\beta_{l,k}}{\sqrt{N}} \sum_{p=1}^N a(\theta_{l,k,p}, \phi_{l,k,p}) \quad (4)$$

In this context, P is the number of multipath components received by the AP from the UE, while $\beta_{l,k} = d^{-\alpha}$ represents the channel response. Here, d is the distance between the UE and the AP, and α is the path loss exponent. The term $(\theta_{l,k,p}, \phi_{l,k,p})$ corresponds to the array steering vector of the AP, associated with the 2D-DOA azimuth angle $0 \leq \theta_{l,k,p} \leq \pi$ and the elevation angle $0 \leq \phi_{l,k,p} \leq \pi$. Furthermore, $(\theta_{l,k,p}, \phi_{l,k,p})$ is specified for each antenna element (m_x, m_y) on the AP, as described in [13].

$$a(\theta_{l,k,p}, \phi_{l,k,p}) = \frac{1}{\sqrt{M}} e^{j((m_x-1)u_{l,k,p} + (m_y-1)v_{l,k,p})} \in \mathbb{C}^{M \times 1} \quad (5)$$

Where $m_x = 1, 2, \dots, M_x, m_y = 1, 2, \dots, M_y \in \mathbb{C}^{M \times 1}$

$$u_{l,k,p} = \left(\frac{2\pi}{d}\right) \cos \theta_{p,l,k} \sin \phi_{p,l,k} \quad (6)$$

$$v_{l,k,p} = \left(\frac{2\pi}{d}\right) \sin \theta_{p,l,k} \sin \phi_{p,l,k} \quad (7)$$

$$a(u_{l,k,p}) = [1, e^{ju_{p,l,k}}, \dots, e^{j(m_x-1)u_{p,l,k}}] \quad (8)$$

$$\hat{h}_{l,k} = \frac{\beta_{l,k}^2}{N} \sum_{p=1}^N E \{a_{l,k,p} a_{l,k,p}^H\} \left(\frac{\beta_{l,i}^2}{M} \sum_{p=1}^M \sum_{i=1, i \neq k}^K E \{a_{l,i,p} a_{l,i,p}^H\} + \sigma^2 I_M \right)^{-1} y_l^p \quad (14)$$

$$a(v_{l,k,p}) = [1, e^{jv_{p,l,k}}, \dots, e^{j(m_y-1)v_{p,l,k}}] \quad (9)$$

B. Channel Estimation

For channel estimation, each access point (AP), in collaboration with distributed CPUs, conducts local channel estimation. It is assumed that the user equipment (UEs) are either stationary or moving at low velocities, resulting in uniform shadowing and path loss conditions. The APs estimate the channels by correlating the received signals with their respective pilot sequences. Due to the high density of UEs within the coverage area and the limited number of available pilot sequences, pilots are reused among multiple UEs, causing inter-cell interference, which serves as the primary source of pilot contamination. To evaluate the performance of cell-free Massive-MIMO systems, the APs correlate \mathbf{Y}_l with the pilot sequence assigned to the k^{th} UE, producing the processed received pilot signal $y_l^p \in \mathbb{C}^M$, represented as:

$$y_l^p = \mathbf{s}_k^H \mathbf{Y}_l = \sqrt{t_u p_{l,k}} \mathbf{s}_{l,k}^H \mathbf{s}_{l,k} h_{l,k} + \sum_{i=1, i \neq k}^K \sqrt{t_u p_{l,i}} \mathbf{s}_{l,i}^H \mathbf{s}_{l,i} h_{l,i} + N_s \in \mathbb{C}^{M \times 1} \quad (10)$$

In Equation (10), the first term corresponds to the desired signal, while the second term represents the impact of uplink pilot contamination. The noise component is denoted as $N_s = \mathbf{s}_k^H \mathbf{N}_l \in \mathbb{C}^{M \times 1}$. The channel estimation error is expressed as $\tilde{h}_{l,i} = h_{l,i} - \hat{h}_{l,i}$. The minimum mean square error (MMSE) estimate for $h_{l,k}$ is computed using the vector $\hat{h}_{l,k}$, as shown below, as detailed in [3] and [14].

$$\hat{h}_{l,k} = R_{l,k} \varepsilon_{l,i} y_l^p \quad (11)$$

and $\varepsilon_{l,i}$ have defined as

$$\varepsilon_{l,i} \triangleq \left(\sum_{i=1, i \neq k}^K s_{l,i} R_{l,i} + \sigma^2 I_M \right)^{-1} \quad (12)$$

where $\sigma^2 I_M$ is element-wise variance with unity matrices. $\mathbf{R}_{l,k} = E \{ \mathbf{h}_{l,k} \mathbf{h}_{l,k}^H \} \in \mathbb{C}^{M \times M}$ is channel covariance matrices and by applying the channel model in Eq. (4) we get

$$R_{l,k} = \frac{\beta_{l,k}^2}{N} \sum_{p=1}^N E \{ a(\theta_{l,k,p}, \phi_{l,k,p}) a(\theta_{l,k,p}, \phi_{l,k,p})^H \} \quad (13)$$

By setting $\mathbf{a}_{l,k,p} = a(\theta_{l,k,p}, \phi_{l,k,p})$, the combination of Equation (11) and Equation (13) results in the following expression:

III. PROPOSED DOA BASED ZF PRECODING

It is assumed that downlink pilot signals are beamformed to user equipment (UEs) utilizing Zero-Forcing (ZF) precoding. As a result, each access point (AP) in the cell-free Massive-MIMO architecture delivers payload data to its associated UE via ZF precoding, represented mathematically as follows:

$$\mathbf{X}_{l,k} = \sum_{k=1}^K w_{l,k} x_{l,k} \quad (15)$$

The variable $x_{l,k}$ denotes the payload data transmitted with allocated power $\rho_{l,k} = \frac{p}{M d_k^\alpha}$, where p is the downlink power, M represents the number of transmitting access points (APs), d_k is the separation between the access point (AP) and the target UE, and α is the path loss exponent. The transmission is performed using the precoding vector $w_{l,k} \in \mathbb{C}^{M \times 1}$, designed to optimize the spatial direction of the signal. This vector satisfies the normalization conditions $\mathbf{E} \|w_{l,k}\| = 1$ and $\mathbf{E} \|w_{l,k} x_{l,k}\|^2 = \rho_{l,k}$.

The reciprocity of uplink and downlink channels within the coherence block enables the CPU to utilize uplink channel estimates to compute optimal downlink precoding vectors. The intended signal for user equipment k travels via the precoding channel as $(\mathbf{h}_{l,k})^H w_{l,k}$. While UE k may lack prior knowledge of the precoding channel, it can estimate it from the received downlink signal or the mean value $E\{(\mathbf{h}_{l,k})^H w_{l,k}\}$. Consequently, the received signal at user k within a cell-free Massive-MIMO framework can be expressed as follows [15,16]:

$$y_{l,k} = \sum_{l=1}^L E\{(\mathbf{h}_{l,k})^H w_{l,k}\} x_{l,k} + \sum_{l=1}^L \sum_{i=1, i \neq k}^K E(\mathbf{h}_{l,i})^H w_{l,i} x_{l,i} + n_k \quad (16)$$

In TDD mode, the reciprocal nature of uplink and downlink channels establishes a seamless connection between uplink channel estimation and the development of effective downlink precoding strategies. Leveraging this concept, a novel precoding approach for cell-free Massive-MIMO systems is introduced, utilizing Direction of Arrival (DOA) data to create multiple beams directed in both azimuth and elevation planes. This approach takes advantage of the uplink-downlink duality property, as outlined in [3, 10, 11], which reflects the strong correlation between downlink and uplink spectral efficiencies. This duality enables the design of Zero-Forcing (ZF) downlink precoding, where the weighting vectors $w_{l,k}$ can be expressed as follows:

$$w_{l,k} = \frac{v_{l,k}}{\sqrt{\mathbf{E}\{\|v_{l,k}\|^2\}}}, \quad (17)$$

and $v_{l,k} = \hat{H}_{l,k} (\hat{H}_{l,k}^H \hat{H}_{l,k})^{-1}$

Here, $\hat{H}_{l,k} = [\hat{h}_{l,1}, \dots, \hat{h}_{l,K}] \in \mathbb{C}^{M \times K}$ is rank-deficient. Each access point (AP) detects the desired UE's signal by employing the linear receive combining vector $v_{l,k}^H$. The access point (AP) determines the combining vector for the k th UE using channel estimates derived during the pilot transmission phase. During the data transmission process, APs within the cell-free Massive-MIMO system correlate the received signal y_l^p from Equation (10) with the selected combining vector, resulting in the following expression:

$$v_{l,k}^H y_l^p = v_{l,k}^H \hat{h}_{l,k} s_{l,k} + v_{l,k}^H \hat{h}_{l,k} s_{l,k} + \sum_{i=1, i \neq k}^K v_{l,k}^H \hat{h}_{l,i} s_{l,i} + v_{l,k}^H n_l \quad (18)$$

In Equation (10), The first term on the right-hand side represents the desired signal transmitted via the estimated channel, while the second term corresponds to the desired signal passing through the unestimated channel. The third term accounts for intra-cell interference. The Zero-Forcing combining vector, indicated as $v_{l,k}$, is derived following the formulations in [3], [10].

$$v_{l,k} = p_{l,k} \left(\sum_{i=1}^K p_{l,i} (\hat{h}_{l,i} \hat{h}_{l,i}^H) \right)^{-1} \hat{h}_{l,k} \quad (19)$$

By combining Equations (11) and (13) and substituting them into Equation (19), the resulting relation can be represented as:

$$v_{l,k} = \frac{\beta_{l,i}^2}{M} \left(\sum_{p=1}^M p_{l,i} E\{a_{l,i} a_{l,i}^H\} \right)^{-1} \frac{\beta_{l,k}^2}{N} \sum_{p=1}^N E\{a_{l,k} a_{l,k}^H\} \quad (20)$$

A. Impact of spatial correlation on pilot contamination

The correlation of spatial channels significantly improves estimation precision, especially under the influence of pilot contamination. This effect ensures that multipath components with a Direction of Arrival (DOA) outside the target UE's DOA region are projected into the orthogonal complement of its covariance matrix, particularly when a large array of antenna elements is utilized (i.e. $(E\{a_{l,i} a_{l,i}^H\})^{-1} E\{a_{l,k} a_{l,k}^H\}$ for $M \rightarrow \infty$) in Eq.(20).

Utilizing the spatial characteristics of transmitted signals allows for the distinction between correlated channels, even under conditions of pilot contamination, thereby mitigating its effects. This is illustrated by defining the steering vector $a(\psi_{i,k}, \varphi_{i,k})$ for the interfering user's signal. Although sharing the same pilot sequence, the azimuth angle $\psi_{i,k} \notin [\theta_{l,k}^{min}, \theta_{l,k}^{max}]$ and the elevation angle $\varphi_{i,k} \notin [\phi_{l,k}^{min}, \phi_{l,k}^{max}]$. Consequently, $a_{l,i}$ and $a_{l,k}$ can be spatially differentiated by using Equation (13). Let us first define $u = \frac{a(\psi_{i,k}, \varphi_{i,k})}{\sqrt{M}} \in \mathbf{R}_{l,k}$, then we have:

$$v_{l,k} = \frac{\beta_{l,i}^2}{M} \left(\sum_{p=1}^M p_{l,i} E\{a_{l,i} a_{l,i}^H\} \right)^{-1} \frac{\beta_{l,k}^2}{N} \sum_{p=1}^N E\{a_{l,k} a_{l,k}^H\} \quad (21)$$

Where $a_{i,k} = a(\psi_{i,k}, \varphi_{i,k})$, $a_{l,k} = a(\theta_{l,k}, \phi_{l,k})$ and $\theta_{l,k}, \phi_{l,k}$ $\psi_{i,k}, \varphi_{i,k}$ have the PDF $n_j(\theta_{l,k}, \phi_{l,k})$, $m_i(\psi_{i,k}, \varphi_{i,k})$ for all paths $i=1, \dots, N$. and $j=1, \dots, M$. Based on the total of a geometric progression, particularly when the array comprises numerous antenna elements, Equation (19) approaches zero, as demonstrated in [10]. Consequently,

$$\frac{1}{NM} E\left\{ \left| a(\psi_{i,k}, \varphi_{i,k})^H a(\theta_{l,k}, \phi_{l,k}) \right|^2 \right\} = 0 \quad (22)$$

The equation underscores that the performance of covariance-assisted channel estimation is heavily influenced

by the degree of intersection between the signal subspaces of the covariance matrices corresponding to the desired and interfering channels. The probability of significant overlap is minimal since both azimuth and elevation angles of arrival are estimated instead of relying on a single angular parameter [17]. This differentiation highlights the critical role that spatial properties of the transmitted signals play in reducing the impact of pilot contamination.

The mathematical expression for the combining vector will now be developed using the azimuth and elevation angles. This formulation is crucial for determining the weighting vectors used in the proposed precoding scheme. By incorporating Equations (6, 7, 8, and 9) into Equation (22), we obtain:

$$\begin{aligned} & \frac{\beta_{l,k}^2}{NM} \sum_{p=1}^N E \{ a_{l,k} a_{l,k}^H \} \\ &= \frac{\beta_{l,k}^2}{NM} \sum_{p=1}^N E \left\{ |a_{l,k}^H(u_{l,k,p}) a_{l,k}(v_{l,k,p})|^2 \right\} \end{aligned} \quad (23)$$

In large-scale implementations with a substantial number of access points (i.e. $M \rightarrow \infty$), the mean channel gain is derived, incorporating the summation form of a geometric progression as presented in [10], can be expressed as in Eq. (24) where $M = M_x M_y$.

Substituting Eq. (25), and Eq. (22) in Eq. (20), the relationship of combining vector $v_{l,k}$ can be written as:

$$SINR_{l,k} = \frac{|\sum_{l=1}^L \sqrt{\rho_{l,k}} E \{ (\mathbf{h}_{l,k})^H w_{l,k} \}|^2}{|\sum_{l=1}^L \sum_{i=1, i \neq k}^K E \sqrt{\rho_{l,i}} (\mathbf{h}_{l,i})^H w_{l,i}|^2 - |\sum_{l=1}^L \sqrt{\rho_{l,k}} E \{ (\mathbf{h}_{l,k})^H w_{l,k} \}|^2 + 1} \quad (29)$$

$$\begin{aligned} E \{ |h_{l,k}|^2 \} &= \frac{\beta_{l,k}^2}{N} \sum_{p=1}^N E \left\{ |a_{l,k}^H(u_{l,k,p}) a_{l,k}(v_{l,k,p})|^2 \right\} \\ &= \frac{\beta_{l,k}^2}{NM} \int_{v'}^v \int_{u'}^u \left| \sum_{m_x}^{M_x-1} \sum_{m_y}^{M_y-1} e^{j2\pi(m_x-1)(m_y-1)(\cos u_{l,k} - \cos v_{l,k})} \right|^2 n(\theta_{l,k}, \phi_{l,k}) dudv \end{aligned} \quad (24)$$

$$E \{ |h_{l,k}|^2 \} = E \left\{ \left| \sum_{m_x=1}^{M_x} e^{2\pi j(m_x-1) \cos \theta_{l,k} \sin \phi_{l,k}} \right|^2 \left| \sum_{m_y=1}^{M_y} e^{2\pi j(m_y-1) \sin \theta_{l,k} \sin \phi_{l,k}} \right|^2 \right\} \quad (25)$$

$$\approx \frac{1}{M} \frac{1 - \cos(M_x \cos(\theta_{l,k} - \hat{\theta}_{l,k}) \sin(\phi_{l,k} - \hat{\phi}_{l,k}))}{1 - \cos(\cos(\theta_{l,k} - \hat{\theta}_{l,k}) \sin(\phi_{l,k} - \hat{\phi}_{l,k}))} \frac{1 - \cos(M_y \sin(\theta_{l,k} - \hat{\theta}_{l,k}) \sin(\phi_{l,k} - \hat{\phi}_{l,k}))}{1 - \cos 2(\sin(\theta_{l,k} - \hat{\theta}_{l,k}) \sin(\phi_{l,k} - \hat{\phi}_{l,k}))}$$

$$v_{l,k} = \frac{p_{l,k}}{MN} \frac{1 - \cos(M \zeta_{l,k})}{1 - \cos(\cos \zeta_{l,k})} \frac{1 - \cos(M \tilde{\zeta}_{l,k})}{1 - \cos(\tilde{\zeta}_{l,k})} \quad (26)$$

$$\zeta_{l,k} = \cos(\theta_{l,k} - \hat{\theta}_{l,k}) \sin(\phi_{l,k} - \hat{\phi}_{l,k}) \quad (26-a)$$

$$\tilde{\zeta}_{l,k} = \sin(\theta_{l,k} - \hat{\theta}_{l,k}) \sin(\phi_{l,k} - \hat{\phi}_{l,k}) \quad (26-b)$$

Therefore, the precoding weighting vector $w_{l,k}$ can be formulated as a function of the estimated elevation and azimuth angles of arrival, in accordance with Equation (17), as follows:

$$\begin{aligned} & w_{l,k} \\ &= \frac{p_{l,k}}{MN} \frac{1 - \cos(M \zeta_{l,k})}{1 - \cos(\cos \zeta_{l,k})} \frac{1 - \cos(M \tilde{\zeta}_{l,k})}{1 - \cos(\tilde{\zeta}_{l,k})} \\ &= \sqrt{\left| \frac{p_{l,k}}{MN} \frac{1 - \cos(M \zeta_{l,k})}{1 - \cos(\cos \zeta_{l,k})} \frac{1 - \cos(M \tilde{\zeta}_{l,k})}{1 - \cos(\tilde{\zeta}_{l,k})} \right|^2} \end{aligned} \quad (27)$$

B. Achievable Downlink Spectral Efficiency Analysis

Using the same approach as outlined in [10], a closed-form expression for the achievable sum rate is presented, taking into consideration errors in channel estimation for both azimuth and elevation DOA, along with the impact of pilot contamination. The achievable sum rate can be expressed as follows:

$$SE = \sum_{l=1}^L \sum_{k=1}^K \frac{t_{d,k}}{t_{c,k}} \mathbf{E} \{ \log_2(1 + SINR_{l,k}) \} \quad (28)$$

Where $SINR_{l,k}$ denotes the signal-to-interference-and-noise ratio (SINR), which is characterized as outlined in Eq. (29). The initial component in the denominator accounts for intra-cell interference. Moreover, in the cell-free Massive-MIMO system, each AP independently determines its beamforming vectors based on its respective channel estimations, $\hat{\mathbf{h}}_{l,k}$ with the assistance of multiple decentralized CPUs.

Maximizing $SINR_{l,k}$ with respect to the estimated 2D-DOA results in a proportional enhancement of $SINR_{l,k}$ for each user, while adhering to the constraints on the total transmit power of AP l remains within specified limits. This dependency is mathematically defined through the precoding vectors outlined in Equation (29) as:

$$\begin{aligned} & \arg \max_{(\hat{\theta}_{l,k}, \hat{\phi}_{l,k})} SE(\theta, \phi) \\ & s. t. \sum_{k=1}^K \|\mathbf{w}_{l,k}\| \leq \rho \end{aligned} \quad (30)$$

Instead of relying on the computational complexity of convex optimization in Equation (30) to calculate all precoding vectors across the network, the system leverages

the principle of uplink-downlink reciprocity. This approach allows the application of the MMSE combining vector, refined using downlink-determined 2D-DOA and regulated power distribution. Given the reciprocity of uplink and downlink channels within the coherence interval, APs utilize uplink channel estimations to calculate and implement suitable beamforming weight vectors, benefiting from the uplink-downlink duality. By exploiting this property, The efficiency of cell-free Massive-MIMO systems can be assessed comprehensively using the Zero-Forcing combining vector, optimized for downlink 2D-DOA estimates. Substituting Equations (27) and (29) into Equation (28) yields the ultimate expression for the lower bound on the achievable rate for user k within the cell-free Massive-MIMO framework.

$$SE = \sum_{l=1}^L \sum_{k=1}^K t_{d,k} E \left\{ \log_2 \left(1 + \frac{CB_{l,k}}{\sum_{i=1, i \neq k}^K [UI_{l,i}] - CB_{l,k}} \right) \right\} \quad (31)$$

$$CB_{l,k} = \frac{\frac{p_{l,k}}{MN} \frac{1 - \cos(M\zeta_{l,k})}{1 - \cos(\cos \zeta_{l,k})} \frac{1 - \cos(M\tilde{\zeta}_{l,k})}{1 - \cos(\tilde{\zeta}_{l,k})}}{\sqrt{\left\| \frac{p_{l,k}}{MN} \frac{1 - \cos(M\zeta_{l,k})}{1 - \cos(\cos \zeta_{l,k})} \frac{1 - \cos(M\tilde{\zeta}_{l,k})}{1 - \cos(\tilde{\zeta}_{l,k})} \right\|^2}} \quad (31-a)$$

$$UI_{l,i} = \frac{\frac{p_{l,i}}{MN} \frac{1 - \cos(M\zeta_{l,i})}{1 - \cos(\cos \zeta_{l,i})} \frac{1 - \cos(M\tilde{\zeta}_{l,i})}{1 - \cos(\tilde{\zeta}_{l,i})}}{\sqrt{\left\| \frac{p_{l,i}}{MN} \frac{1 - \cos(M\zeta_{l,i})}{1 - \cos(\cos \zeta_{l,i})} \frac{1 - \cos(M\tilde{\zeta}_{l,i})}{1 - \cos(\tilde{\zeta}_{l,i})} \right\|^2}} \quad (31-b)$$

Based on the spectral efficiency in Equation (31), it is evident that the uplink combining vectors are utilized in the downlink process to evaluate the precoding vectors, which rely on information from the elevation and azimuth angles. Accurate estimation of the 2D-DOA, encompassing both azimuth and elevation angles of the uplink signals, is essential for achieving optimal performance in cell-free Massive-MIMO systems, where $\theta_{l,k} = \hat{\theta}_{l,k}$ and $\phi_{l,k} = \hat{\phi}_{l,k}$. The spectral efficiency of deterministic Zero-Forcing precoding, which ignores pilot contamination, is used as a reference according to Equation (31). The system model is further verified during downlink transmission by employing the proposed Zero-Forcing precoding technique outlined in Equation (20), which integrates power control to fine-tune the precoding weight vectors. The performance of this method, incorporating power control, is benchmarked against the deterministic Zero-Forcing results derived from Equation (31), with consistency observed between the outcomes. Consequently, the third objective is accomplished by utilizing Equation (31) is utilized to evaluate the performance of the 2D-DOA-based Zero-Forcing precoding method within cell-free Massive-MIMO systems.

IV. SIMULATION RESULTS

This section presents simulation findings evaluating the spectral efficiency of the proposed precoding technique based on 2D-DOA within a cell-free Massive-MIMO framework. The simulation covered a 1 km \times 1 km hexagonal area with 100 APs, each armed with either 4 or 8 antennas, and served

between 40 and 100 user equipment (UEs) randomly distributed across the region. While orthogonal pilot sequences were generated for the UEs, pilot reuse was introduced to account for real-world limitations.

To model spatial correlation and analyze the effects of pilot contamination, a Gaussian local scattering model with a 10-degree angular spread was used. Users with overlapping pilot sequences were either included or excluded from the service. The study introduced a 2D-DOA-based Zero-Forcing precoding technique to address pilot contamination, utilizing 2D-USPRIT and 2D-Fourier Domain Line Search MUSIC for direction-of-arrival (DOA) estimation. Performance comparisons with deterministic Zero-Forcing precoding validated the proposed approach against existing Zero-Forcing methods, showing consistent outcomes. An analysis of key parameters and metrics, including spectral efficiency, highlighted the effectiveness of the 2D-DOA-based approach in mitigating pilot contamination and supporting high-density user environments. A summary of the simulation parameters is provided in Table 1.

TABLE I. SIMULATION PARAMETERS

Parameter	Value	Parameter	Value
Network layout	Hexagonal Topology	Number of multipaths	$N=50$
Carrier frequency	$f_c = 2$ GHz	Network area	1km \times 1km
Cell diameter	300 m	Number of APs	$M = 100$
Number of antenna per AP	$N = 4, 8$	Number of UEs	$K = 40, 100$
Uplink transmit power	$p_{l,k} = 10$ mw	Downlink transmit power	$\rho = 200$ mw
Samples per coherence block	$\tau_c = 200$	Shadow fading (Standard deviation)	$\sigma_{ul} = 8$
APs height to Users	10 m	Users' height	1.5 m
Path loss exponent	$\alpha = 3.8$	-	-

Initially, the received signals for each UE were analyzed to calculate their respective elevation and azimuth angles using 2D-DOA estimation techniques. The cell-free Massive-MIMO system's performance was evaluated by implementing the Zero-Forcing combining vector optimized with accurate downlink 2D-DOA estimates. To quantify this performance, Equation (31) was employed to determine the downlink spectral efficiency.

Figures 1 and 2 illustrate the cumulative distribution function (CDF) representing the downlink spectral efficiency for each user in the cell-free Massive-MIMO system. CDF depends on factors such as the random distribution of access points (APs) and UEs and the precision of the estimated azimuth and elevation DOA angles. Spectral efficiency calculations were performed for multiple precoding methods, including 2D-USPRIT-based Zero-Forcing precoding, 2D-FDLMS-based Zero-Forcing precoding, deterministic Zero-Forcing precoding, and cell-free Massive-MIMO under pilot contamination (PC). The deterministic spectral efficiency of Zero-Forcing precoding without accounting for pilot contamination was used as a baseline for comparison, as outlined in Equation (31).

Figures 1 and 2 illustrate two scenarios: one with 40 UEs, 100 APs, and 4 antennas per AP, and another with 100 UEs, 100 APs, and 4 antennas per AP. In both cases, the proposed 2D-USPRIT-based precoding method achieves the highest spectral efficiency, surpassing the 2D-FDLMS-based approach in mitigating interference. Notably, the performance

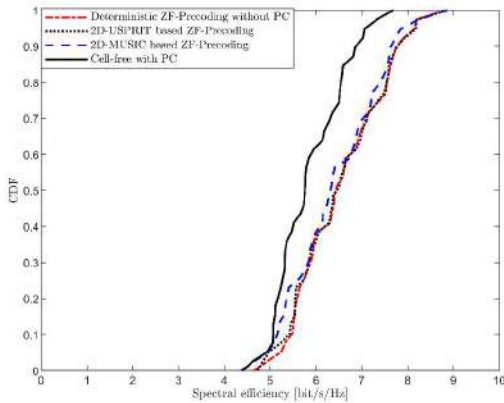


Fig. 1. CDF of downlink spectral efficiency per UE (with $k=40$ UEs and $M=100$, $N=4$ per AP)

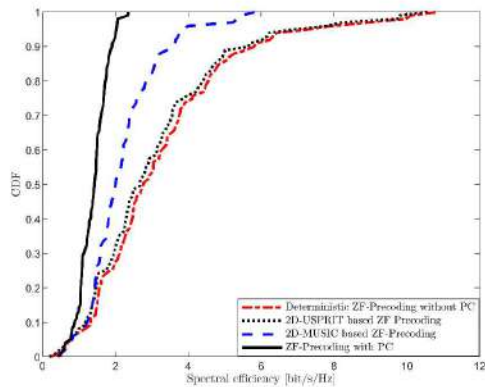


Fig. 2. CDF of downlink spectral efficiency per UE (with $k=100$ UEs and $M=100$, $N=4$ per AP)

of the 2D-USPRIT method closely aligns with that of the deterministic Zero-Forcing method. When the number of UEs increases to 100, as shown in Figure 3, the 2D-USPRIT approach maintains stable performance with minimal impact from the increased user density. In comparison, the 2D-FDLMS-based precoding and pilot-contaminated systems exhibit noticeable degradation, achieving only 87.5% and 80.7% of the deterministic performance, respectively. This highlights the robustness of the 2D-USPRIT method in managing high user densities within cell-free Massive-MIMO systems.

V. CONCLUSION

This study introduces a 2D-DOA-based precoding approach designed to address pilot contamination challenges in cell-free Massive-MIMO systems. The approach combines MMSE channel estimation with 2D-DOA methods, utilizing the spatial properties of uplink signals to significantly reduce interference. A novel mathematical framework for computing receives combining vectors, based on the two-dimensional direction of arrival, forms the foundation for an optimized downlink precoding strategy. The performance of two 2D-DOA estimation techniques, 2D-USPRIT and 2D-FDLMS, was evaluated for spectral efficiency and benchmarked against systems affected by pilot contamination as well as deterministic Zero-Forcing precoding. Among these, the 2D-USPRIT approach exhibited outstanding performance, particularly in scenarios with high user densities, highlighting its potential as an effective solution for mitigating pilot contamination in future 6G networks.

- [1] E. Ali, M. Ismail, R. Nordin, and N. F. Abdulah, "Beamforming techniques for massive MIMO systems in 5G: overview, classification, and trends for future research," *Frontiers of Information Technology & Electronic Engineering*, vol. 18, no. 6, pp. 753-772, 2017.
- [2] M. Balfaqih, Z. Balfaqih, V. Shepelev, S. A. Alharbi, and W. A. Jabbar, "An analytical framework for distributed and centralized mobility management protocols," *Journal of Ambient Intelligence and Humanized Computing*, vol. 13, no. 7, pp. 3393-3405, 2022.
- [3] E. Björnson, J. Hoydis, and L. Sanguinetti, "Massive MIMO networks: Spectral, energy, and hardware efficiency," *Foundations and Trends® in Signal Processing*, vol. 11, no. 3-4, pp. 154-655, 2017.
- [4] H. Q. Ngo, A. Ashikhmin, H. Yang, E. G. Larsson, and T. L. Marzetta, "Cell-free massive MIMO versus small cells," *IEEE Transactions on Wireless Communications*, vol. 16, no. 3, pp. 1834-1850, 2017.
- [5] Y. Zhang, H. Cao, P. Zhong, C. Qi, and L. Yang, "Location-based greedy pilot assignment for cell-free massive MIMO systems," in *2018 IEEE 4th International Conference on Computer and Communications (ICCC)*, pp. 392-396. IEEE, 2018.
- [6] M. Attarifar, A. Abbasfar, and A. Lozano, "Random vs structured pilot assignment in cell-free massive MIMO wireless networks," in *2018 IEEE International Conference on Communications Workshops (ICC Workshops)*, pp. 1-6. IEEE, 2018.
- [7] J. Zheng, J. Zhang, J. Cheng, V. C. Leung, D. W. K. Ng, and B. Ai, "Asynchronous cell-free massive MIMO with rate-splitting," *IEEE Journal on Selected Areas in Communications*, vol. 41, no. 5, pp. 1366-1382, 2023.
- [8] V. M. Palhares, A. R. Flores, and R. C. De Lamare, "Robust MMSE precoding and power allocation for cell-free massive MIMO systems," *IEEE Transactions on Vehicular Technology*, vol. 70, no. 5, pp. 5115-5120, 2021.
- [9] L. Miretti, E. Björnson, and D. Gesbert, "Team MMSE precoding with applications to cell-free massive MIMO," *IEEE Transactions on Wireless Communications*, vol. 21, no. 8, pp. 6242-6255, 2022.
- [10] E. Ali, M. Ismail, N. F. Abdullah, R. Nordin, M. Balfaqih, I. Shglouf, and M. H. Mazlan, "Two dimension angle of arrival-based precoding for pilot contamination reduction in multi-cell massive MIMO systems," *Wireless Networks*, vol. 26, pp. 4129-4147, 2020.
- [11] Ö. T. Demir, E. Björnson, and L. Sanguinetti, "Foundations of user-centric cell-free massive MIMO," *Foundations and Trends® in Signal Processing*, vol. 14, no. 3-4, pp. 162-472, 2021.
- [12] H. L. Yin, Cottatellucci, D. Gesbert, R. R. Müller, and G. He, "Robust pilot decontamination based on joint angle and power domain discrimination," *IEEE Transactions on Signal Processing*, vol. 64, no. 1, pp. 2990-3003, 2016.
- [13] A. Hu, "DOA-based beamforming for multi-cell massive MIMO systems," *Journal of Communications and Networks*, vol. 18, no. 5, pp. 735-743, 2016.
- [14] G. Interdonato, M. Karlsson, E. Björnson, and E. G. Larsson, "Downlink spectral efficiency of cell-free massive MIMO with full-pilot zero-forcing," in *2018 IEEE Global Conference on Signal and Information Processing (GlobalSIP)*, pp. 1003-1007. IEEE, 2018.
- [15] M. Mohammadi, T. T. Vu, H. Q. Ngo, and M. Matthaiou, "Network-assisted full-duplex cell-free massive MIMO: Spectral and energy efficiencies," *IEEE Journal on Selected Areas in Communications*, vol. 41, no. 9, pp. 2833-2851, 2023.
- [16] A. Anand, C. R. Murthy, and R. Chopra, "Impact of mobility on the downlink performance of cell-free massive MIMO systems," *Physical Communication*, vol. 61, pp. 102178, 2023.
- [17] Ali, E., Ismail, M., Nordin, R., & Abdulah, N. F. "Beamforming with 2D-AOA estimation for pilot contamination reduction in massive MIMO," *Telecommunication Systems*, vol. 71, pp. 541-552, 2019.